Fountain Clock Accuracy

Kurt Gibble
The Pennsylvania State University, Department of Physics
State College, PA 16802, USA

***Abstract*—We give a review of recent advances in the accuracy of atomic fountain clocks. The new features are improved experimental and theoretical treatments of distributed cavity phase shifts and a full modeling of microwave lensing. Here we highlight that state selection is often highly non-uniform when Rabi flopping is used instead of an interrupted adiabatic frequency chirp. We show that detuning the state-selection microwave field as well as changing its amplitude can give a much more homogeneous state selection. A spatially inhomogeneous state selection corrupts the density extrapolation because the density distribution changes, which also mixes effects from distributed cavity phase and microwave lensing. This is expected to be important for the microgravity clock PHARAO on ACES, and can also improve fountain clocks.**

I. Introduction

The highest accuracy of atomic fountain clocks has improved by nearly a factor of two over the last two years [1-4]. Significant progress was made by first evaluating distributed cavity phase (DCP) errors [5,6], and secondly, the first full treatments of the biases due to the microwave lensing of atomic wavepackets by the dipole forces in the clocks' Ramsey cavities. DCP errors are fundamentally a Doppler shift that result because the cavities have small traveling waves and the atoms do not exactly retrace their upward and downward fountain trajectories through the clock cavity. Properly evaluating the DCP uncertainty lowered the SYRTE-FO2 uncertainty to 2.8×10^{-16} [1]. With a smaller DCP uncertainty, the microwave lensing uncertainty stood out and a full modeling of it for NPL-CsF2 reduced its uncertainty from 4.1×10^{-16} to 2.3×10^{-16} [2]. The DCP and microwave lensing model was subsequently applied to PTB-CSF2 and the entire SYRTE fountain ensemble, lowering SYRTE-FO2's uncertainty to 2.1×10^{-16} [3,4]. In the next section, we summarize and discuss a recipe to evaluate DCP uncertainties [1-4]. We refer the reader to [2-4] for the treatments of microwave lensing.

With smaller DCP and microwave lensing uncertainties, the frequency shift due to ultracold collisions [7] contributes more prominently to the overall uncertainty of fountains. For many fountains, it is the largest contribution. To extrapolate the clock's frequency to zero density, it is important to change the atomic density without changing the spatial density distribution. One solution is an interrupted adiabatic frequency chirp, which can precisely select half the atoms [8]. A number of clocks are not currently able to use this technique, including the planned PHARAO clock as part of the ACES project [9]. These clocks instead use power-dependent Rabi flopping to change the density. Here we explicitly show that the changing the power gives a large variation in the selection probability, which changes the density distribution. This in turn introduces systematic errors into the density extrapolation, and also convolves it with the systematic DCP and microwave lensing errors. The transverse variation of the selection can be intentionally varied [10] and here we show that detuning the state selection field can give much more homogeneous state selection.

Finally, one of the next largest sources of uncertainty for many clocks is background gas collisions. We briefly discuss these collisions and the differences between room-temperature collisions and the scattering of room-temperature atoms off of ultra-cold atoms.

II. DCP Evaluation

Our models of DCP errors [5,6] were stringently verified with three fountains without any free parameters [1-3]. Here we briefly review and discuss a procedure to evaluate DCP uncertainties.

The key step in our treatment is to decompose the loss fields in the cavities into an azimuthal Fourier series $\cos(m\phi)$ [5,6]. This reduces the calculation of the 3D cavity field near the cavity axis to a sum of 2D finite-element solutions for m=0,1, and 2. Higher m are trivial because the fields are proportional to ρ^m for $\rho\rightarrow0$. This Fourier series also dictates the symmetry of the fountain perturbations that produce DCP shifts.

The m=0 DCP errors are small at optimal microwave amplitude and can be accurately calculated. The m=0 phase variations are predominately longitudinal, which leads to a large dependence of the DCP shift on microwave amplitude. The m=2 DCP shifts are quadrupolar and also quite small, of order 1×10^{-16}. Here, detection laser non-uniformity and the uncertainty in the centering of the cloud's launch point gives the errors. These can also be modeled sufficiently well that conservative limits are adequate.

This work was financially supported by the NASA, NSF, ONR, Penn State, and la Ville de Paris.

978-1-4673-1923-2/12/$31.00 ©2012 IEEE

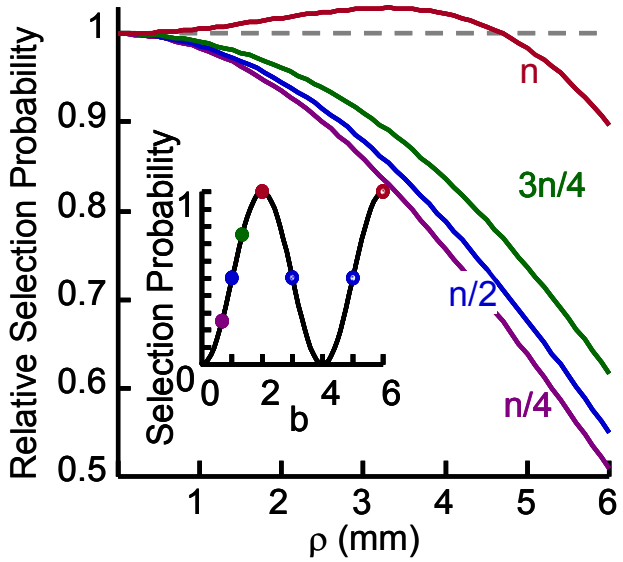

Fig. 1. State selection probability for different pulse areas. For a field on resonance that is not pulsed, the selection probability is $\sin^2(\theta/2)$ where $\theta(\rho)=\theta(\rho=0)J_0(k\rho)$, which is independent of the selection cavity geometry [6]. The inset depicts selecting the various density fractions with several pulse areas.

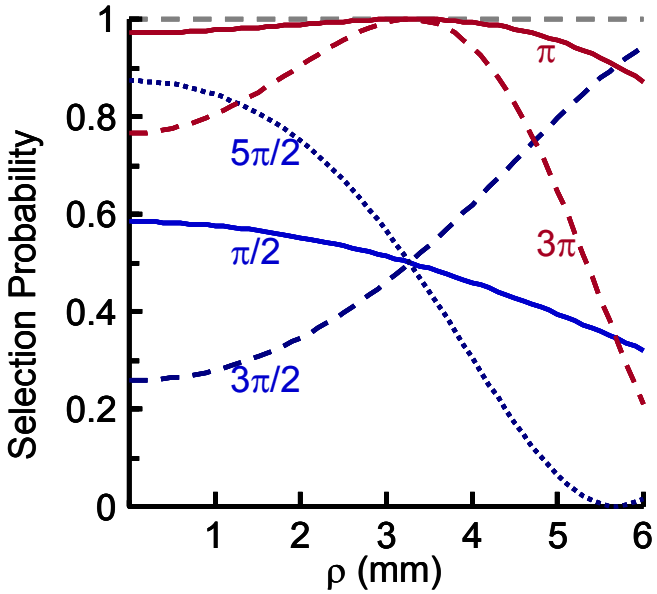

Fig. 2. Changes in the shape of the state selection probability for different pulse areas. Selecting ½ the atoms, $3\pi/2$ pulses give a larger variation with the opposite curvature. Operating the clock alternately with $\pi/2$, $3\pi/2$, and $5\pi/2$ state selection pulses probes the effect of state selection inhomogeneity on the clock's frequency [10].

The m=1 DCP errors are due to phase gradients across the cavity, for example due to imbalances in the power fed from opposite sides of the cavity. These have a large scale size – they can easily be 10^{-14} for a single-sided cavity feed and a fountain tilt of 2 mrad. The clock cavity should be tuned to resonance so that phase imbalances of the feeds do not produce DCP errors [6]. Then, the feeds should be balanced at optimal amplitude so that there is no linear change in fountain frequency when the fountain is tilted to move the atoms along the feed axis [1]. Then, the fountain can be aligned to be vertical, for example by comparing frequency differences between feeding only one feed or the other at different elevated microwave amplitudes [1, 11]. Note that measuring the tilt sensitivity with two $5\pi/2$ pulses does not help to establish the m=1 DCP uncertainty [1,6]. Inhomogeneous cavity surface resistances can give dramatically different microwave amplitude dependences of the DCP shifts.

The fountain can also be tilted to move the atoms perpendicular to the feeds. Here, it is more difficult to be sure of true vertical for m=1 DCP errors [1-4]. For this reason, future cavity designs prefer to have at least 4 independent feeds that are distributed equally in ϕ [6]. Optimizing the feed positions and cavity shape should lead to negligible DCP uncertainties, even at high microwave amplitudes [6].

III. State Selection

Driving a $\pi/2$ pulse on resonance in a state selection cavity is a common way to change the atomic density to evaluate the ultracold collision frequency shift. If the state selection field is applied for the entire traversal of the atoms through the cavity, instead of a short pulse while the atoms are in the middle of the cavity, the transition probability as a function of position is shown in Fig. 1. As illustrated in the inset, all or half of the atoms can be selected with a number of pulse areas, e.g. $\pi/2$, $3\pi/2$, and $5\pi/2$ [10]. Selecting with a $3\pi/2$ instead of a $\pi/2$ pulse reverses the curvature of the selection probability and

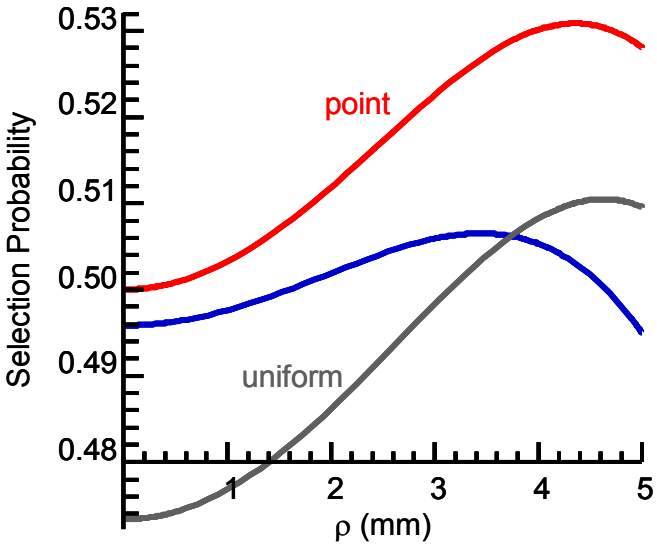

Fig. 3. State selection probability for pulse areas that give a selection probability with the smallest variation (blue), ±1%, and by operating where the transition probability is independent of amplitude for a point source on axis (red), and a uniform density (gray). For these, the detunings are (1.0029, 1.0048, 1.0422) $\Delta\nu_{HWHM}$ and pulse areas (0.7915, 0.8478, 0.8500)π. Here we use the PTB-CSF2 clock cavity as an example. Thus, these results include the mode perturbations due to the holes in the cavity endcaps.

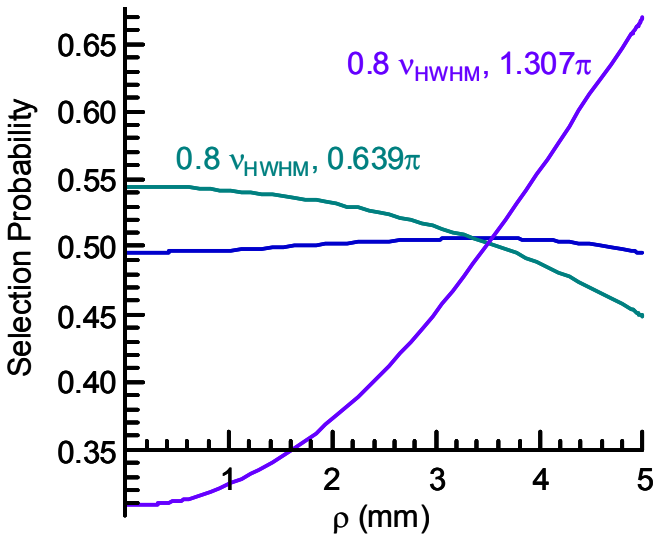

Fig. 4. The selection inhomogeneity can be intentionally increased by a modest amount. Detuning to $0.8\Delta\nu_{HWHM}$ and selecting half the atoms gives modest and opposite selection curvatures (aqua and purple). The blue curve is the same as in Fig. 3

also exaggerates the variation as shown in Fig. 2. Using $5\pi/2$ gives even more dramatic variations.

In Fig. 3, we show that the selection probability can be very flat, varying by ±1%, by detuning the selection cavity field to 1.0029 $\Delta\nu_{HWHM}$ and giving a 0.7915 π pulse. Here $\Delta\nu_{HWHM}$ is the half-width at half-maximum of a π pulse for a small cloud of atoms passing through the cavity on axis. (For a uniform cloud, $\Delta\nu_{HWHM}$ is 6.68% wider than for a point source.) In Fig. 3 for reference, we also show the selection probability for the case of a very small cloud launched through the selection cavity and the transition probability maximized with respect to microwave amplitude, where the detuning is set to give a transition probability of ½ (red). Here, the detuning is 1.00484 $\Delta\nu_{HWHM}$ and the pulse area is 0.8478 π. Similarly, for a uniform density distribution, e.g. for a cloud passing downward through the selection cavity, gives 1.04222 $\Delta\nu_{HWHM}$ and 0.8500 π (gray). In essence, by operating such that the transition probability is independent of power and at the detuning that gives the desired density ratio, the selection probability is far more uniform. In Fig. 4, the variation can be easily exaggerated and the shape reversed by choosing different detunings and pulse areas, but with more modest variations than in Fig. 2.

IV. Background Gas Collisions

A number of clocks assign a frequency uncertainty of 1×10^{-16} for collisions with background gas atoms. The coefficients that are used were measured in room-temperature Cs collisions in vapor cell clock [12]. In a fountain, even a small scattering angle with a room-temperature atom or molecule will expel the Cs atom from being detected. The range of scattering angles that are detected are well within the quantum mechanical diffractive scattering cone - only of order 1% of the diffractive cone is detected. Therefore the measured frequency shifting rate coefficients in [12] are not applicable. Further, the interference of the scattered and the unscattered parts of the atoms' wave functions can be expected to dominate the frequency shift cross section. More attention to this systematic error is clearly required.

Acknowledgment

We acknowledge many discussion and contributions from collaborators at LNE-SYRTE, NPL, and PTB, and especially Ruoxin Li at Penn State.

References

[1] J. Guéna, R. Li, K. Gibble, S. Bize, and A. Clairon, "Evaluation of Doppler Shifts to Improve the Accuracy of Primary Atomic Fountain Clocks," Phys. Rev. Lett. vol. 106, 130801 (2011).

[2] R. Li, K. Gibble, K. Szymaniec, "Improved accuracy of the NPL-CsF2 primary frequency standard: evaluation of distributed cavity phase and microwave lensing frequency shifts," Metrologia vol. 48, pp. 283-289, (2011).

[3] S Weyers, V Gerginov, N Nemitz, R Li, K Gibble, "Distributed cavity phase frequency shifts of the caesium fountain PTB-CSF2," Metrologia vol. 49, pp. 82-87, (2012).

[4] J. Guéna, M. Abgrall, P. Laurent, B. Chupin, M. Lours, G. Santarelli, P. Rosenbusch, M. E. Tobar, R. Li, K. Gibble, A. Clairon, and S. Bize, "Progress in atomic fountains at LNE-SYRTE," IEEE Trans. Ultrasonics, Ferroelectrics, and Freq. Control, vol. 59, 391-410 (2012).

[5] R. Li and K. Gibble, "Phase variations in microwave cavities for atomic clocks," Metrologia vol. 41, pp. 376-386 (2004).

[6] R. Li and K. Gibble, "Evaluating and minimizing distributed cavity phase errors in atomic clocks," Metrologia vol. 47, pp. 534-551 (2010).

[7] K. Gibble and S. Chu, "A laser cooled Cs frequency standard and a measurement of the frequency shift due to ultra-cold collisions," Phys. Rev. Lett. Vol. 70, pp. 177-180 (1993).

[8] F. Pereira Dos Santos, H. Marion, S. Bize, Y. Sortais, A. Clairon, and C. Salomon, "Controlling the Cold Collision Shift in High Precision Atomic Interferometry," Phys. Rev. Lett. Vol. 89, 233004 (2002).

[9] P. Laurent et al., "Design of the cold atom PHARAO space clock and initial test results," Appl. Phys. B vol. 84, 683 (2006).

[10] C. Fertig and K. Gibble, "Measurement and cancellation of the cold collision frequency shift in an ^{87}Rb fountain clock," Phys. Rev. Lett. vol. 85, 1622-1625 (2000).

[11] F. Chapelet et al., Proceedings of the 20th European Frequency and Time Forum, 2006 (EFTF, Braunschweig, 2006), p. 160.

[12] C. W. Beer and R. A. Bernheim, "Hyperfine pressure shift of 133Cs atoms in noble and molecular buffer gases," Phys. Rev. A vol. 13, pp. 1052-1057 (1976).